Calculation of near-field scanning optical images of exciton, charged-exciton, and multiexciton wave functions in self-assembled InAs/GaAs quantum dots

Lixin He,[1] Gabriel Bester,[2] Zhiqiang Su,[1] and Alex Zunger[2]
[1]*Laboratory of Quantum Information, University of Science and Technology of China, Hefei, Anhui 230026, People's Republic of China*
[2]*National Renewable Energy Laboratory, Golden, Colorado 80401, USA*
Received 26 February 2007; published 12 July 2007

The near-field scanning optical microscopy images of excitonic wave functions in self-assembled InAs/GaAs quantum dots are calculated using an empirical pseudopotential method, followed by the configuration interaction treatment of many-particle effects. We show the wave functions of neutral exciton X^0 of different polarizations and compare them to those of the biexciton XX^0 and the charged excitons X^+ and X^-. We further show that the exciton X $P_h \rightarrow S_e$ transition which is forbidden in the far-field photoluminescence has intensities comparable to those of X $S_h \rightarrow S_e$ transition in the near-field photoluminescence.

DOI: 10.1103/PhysRevB.76.035313 PACS number s : 73.21.La, 71.35.−y, 78.67.Hc

I. INTRODUCTION

The three-dimensional confinement and nearly perfect isolation from its environment given in self-assembled semiconductor quantum dots QDs lead to "atomlike" electronic structure features manifested, among others, by eV photoluminescence PL linewidths and a long coherence time. Such narrow and isolated levels open the way for potential applications using as single-photon emitters[1] and quantum-entangled sources.[2] At the same time, this allows fundamental studies of eV-scale fine-structure splitting[3,4] of exciton lines due to the electron-hole exchange interaction, spectral shift due to charged excitons,[5–7] as well as multiexciton formation and decay. However, the spatial resolution of the traditional far-field spectroscopy is limited to /2, where is the wavelength of the probing light,[8] much larger than the typical sizes of quantum dots a few tens to about a hundred nanometers . Recently, it became possible to examine the inner structures of an exciton in the QDs and map out its spatial distribution using the near-field scanning optical microscopy NSOM .[9,10] In the far-field measurement, the transition intensity within single-particle approximation is proportional to $\mathbf{p}^2 = \psi_c \mathbf{r} \psi_v^2$, where ψ_c and ψ_v are the conduction and valence band wave functions, respectively. While in the far-field measurements, the extent of the incident electromagnetic wave is such that its magnitude over the entire dot region can be safely taken as constant, in the near field, the electromagnetic profile of the tip $\mathbf{r}-\mathbf{r}_0$, has an extent comparable to the size of the nanostructure and must be explicitly taken into account:

$$E(\mathbf{r}) = (\mathbf{r}-\mathbf{r}_0) E_0. \quad (1)$$

In this case, the transition intensity is modulated by the shape of the external field, i.e., proportional to $\mathbf{p}(\mathbf{r}_0)^2 = \psi_c(\mathbf{r}) (\mathbf{r}-\mathbf{r}_0) \psi_v^2$. The resolution of NSOM can thus be much higher than[9] /2, providing details on how the carriers are distributed in the quantum dots.

In a QD, the electron and hole wave functions can be approximated by products of envelope functions and Bloch functions. In the far-field measurement, the interband transitions obey two kinds of selection rules: one related to the Bloch part of the wave functions and one to the envelope component of the wave functions. For example, from the four possible $S_h \rightarrow S_e$ excitonic transitions, two are bright and two are dark. The dark transitions are forbidden because the total angular momentum from the electron and hole *Bloch functions* parts is 2, and hence cannot be carried out by a single photon. In contrast, all of the eight $P_h \rightarrow S_e$ transitions are forbidden because a photon does not couple effectively to the *envelope* orbital angular momentum of the exciton. However, in NSOM, where the electromagnetic field is applied inhomogeneously only to a part of the dot, the global spatial symmetry is broken, thus altering the selection rules for the envelope functions and allowing transitions that are forbidden in far-field measurement.[11] We show here that the $P_h \rightarrow S_e$ transitions which are far-field forbidden have intensities in NSOM comparable to the $S_h \rightarrow S_e$ transitions. Furthermore, NSOM provides additional far-field allowed information about the Bloch part of the wave functions, which the far-field spectroscopy is lacking. For example, by comparing the transition intensities of different polarizations, one could determine the relative phase between X and Y components of the hole wave functions at each point. In contrast, in the far-field measurements, only the total polarization is measured and the wave function phase information of the Bloch part is lost.

Recently, Matsuda *et al.*[10] have measured the near-field PL image of naturally occurring GaAs QDs formed spontaneously in narrow quantum wells. The enhanced NSOM spatial resolution is as high as 30 nm, much smaller than the measured QD sizes of ~200 nm. Unfortunately, the spatial resolution is limited because of the capping layers and is still too low for the self-assembled InAs/GaAs quantum dots.[12] In this paper, we predict via atomistic pseudopotential method the near-field PL images of the neutral exciton X^0, the biexciton XX^0, and the charged excitons X^+ and X^- in the much smaller self-assembled InAs/GaAs quantum dots, in anticipating future NSOM measurements.

II. METHODS

A. Far-field vs NSOM transition elements

To obtain the NSOM images, one must first calculate the single-particle wave functions for electrons and holes by solving the Schrödinger equations,

$$-\frac{1}{2}\nabla$$

function for the mth band. The envelope functions are slow varying functions, compared to the Bloch functions. We can therefore separate the Bloch functions and envelope functions by dividing the volume into small regions, e.g., the eight-atom unit cells. In each unit cell, the envelope functions $f_m(\mathbf{x})$ and $(\mathbf{r})$ can be treated as constants, i.e.,

$$\mathbf{p}(\mathbf{r}_0) = \int d\mathbf{r}\,\psi_v^*(\mathbf{r})\,\psi_c(\mathbf{r})(\mathbf{r}-\mathbf{r}_0) \approx \sum_{\mathbf{r}_i}\sum_{m,m'} f_m^{*v}(\mathbf{r}_i) f_{m'}^{c}(\mathbf{r}_i)\,\mathbf{d}_{m,m'}(\mathbf{r}_i-\mathbf{r}_0), \quad (13)$$

where $\mathbf{r}_i$ is the position of ith cell and

$$\mathbf{d}_{m,m'} = \frac{1}{V}\int d\mathbf{r} u_{\Gamma,m}^*(\mathbf{r})\,\mathbf{r}\,u_{\Gamma,m'}(\mathbf{r}) \quad (14)$$

is the dipole matrix element between bulk bands. In a periodic system, it is more convenient to use an alternative formula to calculate the dipole,[21]

$$\mathbf{d}_{m,m'} = \frac{1}{im\omega_{m,m'}} u_{\Gamma,m}\hat{\mathbf{p}}\,u_{\Gamma,m'}. \quad (15)$$

If we assume high spatial NSOM resolution, i.e., $\mathbf{r}_i-\mathbf{r}_0 = \mathbf{r}_i-\mathbf{r}_0$, Eq. (13) can be further simplified as

$$\mathbf{p}(\mathbf{r}_0) \approx \sum_{m,m'} f_m^{*v}(\mathbf{r}_0) f_{m'}^{c}(\mathbf{r}_0)\,\mathbf{d}_{m,m'}. \quad (16)$$

Combining Eqs. (10) and (16), we see that the shape of NSOM transition is the sum of the multiband envelope functions of the exciton weighted by the single-particle dipole matrix elements, i.e.,

$$\mathbf{M}^{\alpha}(\mathbf{r}_0) = \sum_{v=1}^{N_v}\sum_{c=1}^{N_c} C_{v,c}^{\alpha}\sum_{m,m'} f_m^{*v}(\mathbf{r}_0) f_{m'}^{c}(\mathbf{r}_0)\,\mathbf{d}_{m,m'}. \quad (17)$$

Previously, the NSOM images have been calculated via single-band EMA.[11,22,23] In this approximation, the dipole moment $\mathbf{d}$ is directly taken from bulk 83u97i.1Tf-23.0=58u2d1Tf-.8453ulk 357.1-31lls,9(EMA.)TJ6.9846006.1845d783u97

whereas the two high energy states $B1$ and $B2$ are allowed by the Bloch part. In the far-field measurement, the P

the 110

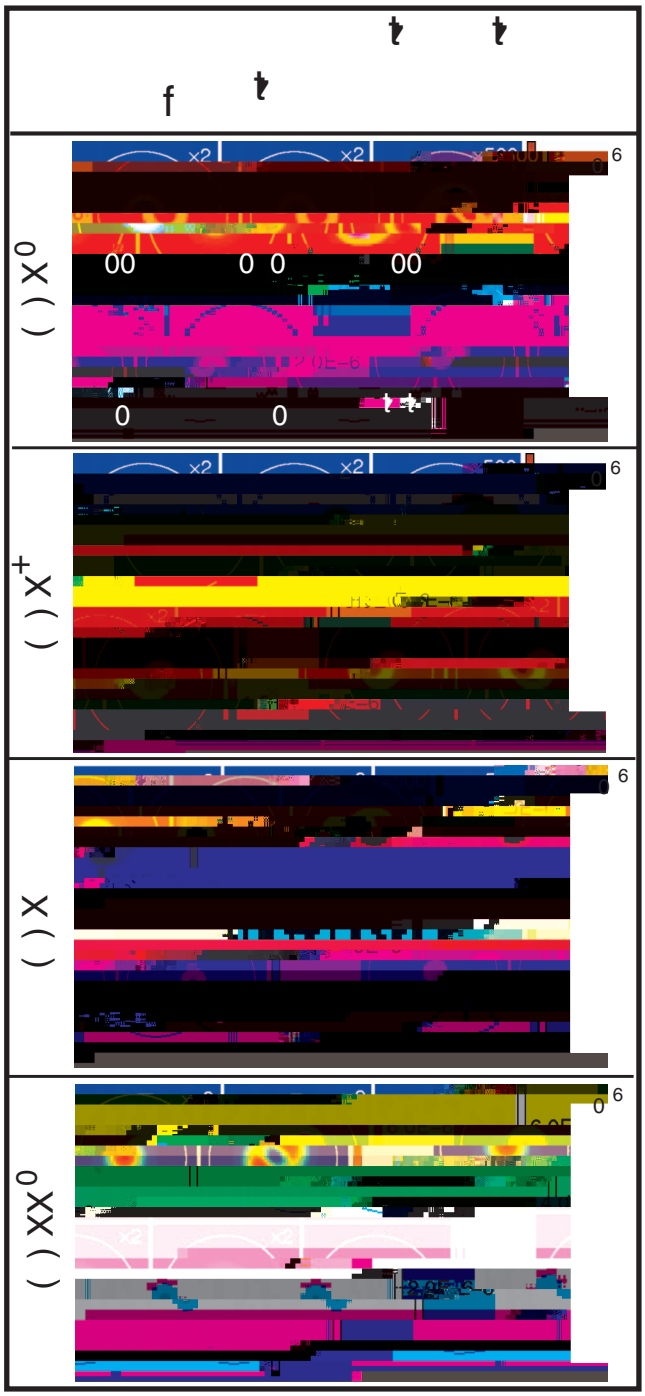

FIG. 4. Color The total NSOM images sum over all fine structures of excitonic $S_h \rightarrow S_e$ transitions see Fig. 1 for a X^0, b X^+, c X^-, and d XX^0 in self-assembled InAs/GaAs QD with b =27.5 nm and h=3.5 nm, calculated from Eq. 17 . The unit of the color bar is arbitrary but equal tco9Do3heb

ger. On the other hand, we ignored the continuum states in the CI calculation which may also underestimate the correlation effects to the wave functions.

IV. SUMMARY

We calculate the NSOM images of exciton complexes in self-assembled InAs/GaAs QD using an atomistic pseudopotential method followed by a configuration interaction treatment of the correlations. The NSOM images reveal the spatial structure of exciton and give information about the Bloch function character of the wave function, which remain unobserved in conventional far-field measurements. We show that the $P_h \rightarrow S_e$ transition, which is forbidden in the far-field PL measurement, has transition intensity comparable to that of the $S_h \rightarrow S_e$ transition in NSOM measurements. We also calculate the NSOM image of charged excitons X^+ and X^- and biexciton XX^0 and compare them with the image of X^0. We found that the images obtained for charged excitons and the biexciton show features very similar to the ones obtained from the exciton decay.

ACKNOWLEDGMENTS

L.H. acknowledges the support from the Chinese National Fundamental Research Program 2006CB921900 , the Innovation funds and “Hundreds of Talents” program from Chinese Academy of Sciences, and the National Natural Science Foundation of China Grant No. 10674124 . The work done at NREL was funded by the U.S. Department of Energy, Office of Science, Basic Energy Science, Materials Sciences and Engineering, LAB-17 initiative, under Contract No. DE-AC36-99GO10337 to NREL.

[1] P. Michler, A. Kiraz, C. Becher, W. V. Schoenfeld, P. M. Petroff, L. Zhang, E. Hu, and A. Imamoğlu, Science **290**, 2282 2000 .
[2] N. Akopian, N. H. Lindner, E. Poem, Y. Berlatzky, J. Avron, D. Gershoni, B. D. Gerardot, and P. M. Petroff, Phys. Rev. Lett. **96**, 130501 2006 .
[3] D. Gammon, E. S. Snow, B. V. Shanabrook, D. S. Katzer, and D. Park, Phys. Rev. Lett. **76**, 3005 1996 .
[4] M. Bayer, A. Kuther, A. Forchel, A. Gorbunov, V. B. Timofeev, F. Schäfer, J. P. Reithmaier, T. L. Reinecke, and S. N. Walck, Phys. Rev. Lett. **82**, 1748 1999 .
[5] A. Hartmann, Y. Ducommun, E. Kapon, U. Hohenester, and E. Molinari, Phys. Rev. Lett. **84**, 5648 2000 .
[6] D. V. Regelman, E. Dekel, D. Gershoni, E. Ehrenfreund429.3E.)er, and D. Park, Phys. Rev. Lett.. M. Petroff,